MISMATCHES APPLIED TO LIGTENBERG'S REFLECTIVE MOIRÉ METHOD

by

Belthur Ranganayakamma
Graduate Student

and

Fu-pen Chiang
Associate Professor

Dept. of Mechanics, State University of N.Y.
at Stony Brook, N.Y.

Report No. 176

September 1970

ABSTRACT

A method is developed whereby the accuracy of Ligtenberg's reflective moiré method for plates can be improved. The method utilizes the linear and rotational mismatches to increase the fringe densities along directions parallel and perpendicular to the grating lines, respectively. As a result greater precision can be obtained in the plotting of curves of partial slopes which are used for determination of curvatures and twists of the flexed plate.

Introduction

The reflective moiré method developed by Ligtenberg [1]* has been widely utilized for the study of bending of plate [2] . The technique is also suitable for two dimensional stress analysis [3]. Ligtenberg originally used a cylindrical screen (grating) for his apparatus. Reider and Ritter [4] modified the technique so that a plane grating could be used. Later it was further modified by Chiang and Treiber [5] to allow continuously variable sensitivity. Essentially the technique consists of projecting a grating onto a mirrored plate surface which when loaded distorts the grating image due to the change of plate curvature. If the grating image before and after loading are superimposed on a piece of film (usually through double exposure technique) a moiré pattern is formed as the result of the interference of the two images. These fringes can be directly interpreted as the contour lines of the slopes of the flexed plate. If the plate before deformation occupies the the x-y plane and we denote w as the deflection in the direction of z, curves representing $\frac{\partial w}{\partial x}$ and $\frac{\partial w}{\partial y}$ can be plotted from the fringes along the sections of interest. Moments and twist can then be obtained by differentiating the curves to obtain $\partial^2 w/\partial x^2$, $\partial^2 w/\partial y^2$, and $\partial^2 w/\partial x \partial y$.

Owing to the inherent inaccuracy associated with graphical or numerical differentiation it is evident that the curves representing $\partial w/\partial x$ and $\partial w/\partial y$ should be drawn as accurately as possible. However there are cases for which the response of the plate may be such that only a few fringes are obtained in the field.As a result accurate plotting is impossible due to the limited points defining the curve. One way to increase the number of fringes in the field is to increase the line density of the grating used.

---

* Numbers in brackets denote references at the end of the paper

However increasing sensitivity usually accompanies the reduction of pattern contrast. Unless aided by special optical techniques such as spatial filtering [6,7], patterns obtained with high density gratings are sometimes not suitable for analysis due to poor contrast. Another problem that comes from high density grating is the creation of a new set of moiré fringes in some region when the fringes are too crowded, and these fringes cannot be interpreted as the contour lines of the slopes. An example is given in Fig. 1 where (a) and (b) show two moiré patterns of a circular plate under uniform pressure*. The load was the same for both patterns. Only the line density of the grating was changed from 9.54 lpi in (a) to 17.7 lpi in (b). It is seen that not only the contrast is poor in pattern (b), but the fringes were so crowded that a new set of fringes were starting to form at the central portion of the plate. These new fringes tend to interfere with the original set and are not easily interpretable in terms of slopes or curvatures of the plate.

In this paper methods of introducing linear and rotational mismatches into the reflective moiré method are presented whereby fringe densities along both x and y directions can be increased without resorting to high density grating or the increase of loading. As a result, curves can be more accurately plotted because of the increase of data points. The technique is analogous to the mismatch method for plane moiré developed by Chiang [8].

*The meaning of Fig. 1-(c) will be evident in the later part of the text.

Different Types of Mismatches

In the following analysis the optical arrangement as introduced by Chiang and Treiber [5] will be used throughout because of its versatility in introducing various types of mismatches. The optical set up is schematically shown in Fig. 2 where a small grating of certain line density is inserted into an ordinary slide projector which projects the magnified grating image on to the ground glass. The grating image is then viewed by a camera via a partial mirror and the reflective model plate surface.

In the plane moiré method for which two gratings are used (one as master grating and one as model grating) mismatches can be easily defined as the difference in pitch* (linear mismatch) or in orientation (rotational mismatch) between the two gratings before the load is applied [8]. In the reflective moiré method however only one grating is used. The superposition is made between the two images reflected back from the mirrored plate surface before and after the loading. In order to define mismatches it is necessary to introduce the following two terms first, namely, grating-before-loading (GBL) and grating-after-loading (GAL). The former is defined as the grating (i.e. its density and orientation) on the ground glass (see Fig. 2) to be viewed by the camera via undeformed plate, and latter is defined as the grating to be viewed via deformed plate. With this nomenclature we can then define the linear mismatch as the difference in pitch between GBL and GAL and the rotational mismatch as the difference in orientation between them. Linear and rotational mismatch can be introduced into the reflective moiré system either separately or simultaneously depending upon the need of the problem. While various amounts of the former can be imposed upon the system by

* pitch is defined as the spacing between two grating lines

changing distance between the ground glass and the projector (see Fig. 2), the latter can be brought in by either tilting the "grating slide" inside the projector or by tilting the projector itself to a proper inclination. If the GBL and GAL are photographed on one piece of film using double exposure technique without any loading being actually applied to the plate the resulting moiré patterns are due to mismatches only. They are patterns of uniformly spaced straight fringes. The orientation of and spacing between these fringes are functions of the type and amount of mismatches introduced. If we use the following notation:

p = pitch of GBL,

p' = pitch of GAL,

θ = acute angle between lines of GBL and GAL,

ϕ = angle of inclination of fringes measured in the same way as θ,

δ = fringe spacing,

it can be shown that they are related by the following equations [10]:

$$\delta = \frac{p\,p'}{\sqrt{p^2\sin^2\theta + (p\cos\theta - p')^2}} \tag{1}$$

$$\phi = \tan^{-1}\frac{p'\sin\theta}{p\cos\theta - p'} \tag{2}$$

Examples of mismatch fringe patterns are shown in Fig. 3 in which (a) (b) and (c) are the moiré patterns due to linear, rotational, and the combination of linear and rotational mismatches, respectively. The magnitude of the mismatches are indicated in the figure by the line densities and orientations. It is useful to note that linear mismatch fringes are parallel to the grating lines, rotational mismatch fringes are perpendicular to the line bisecting the angle θ, and the combinational mismatch fringes are oriented somewhere in between the two extremes.

The Use of Linear Mismatch

The purpose of introducing mismatches is to increase the fringe density where it is needed. In the reflective moiré method fringes represent contour lines of slopes in the direction normal to the grating lines. Thus a flexed plate with constant curvature along a direction will be represented by a pattern of uniformly spaced fringes if the grating is oriented with the lines perpendicular to the direction. The fringes are of course also perpendicular to the direction. Therefore, a linear mismatch moiré pattern such as shown in Fig. 3(a) can be interpreted as representing a fictitious constant curvature field in the direction normal to the grating lines. In order to use linear mismatch effectively it should then be introduced additively rather than subtractively into the needed region. In other words the fictitious curvature should have the same sign as that of the flexed plate at the places of interest. Otherwise the mismatch will not serve its purpose. This point is demonstrated in the following examples. In Fig. 4-(a) a moiré pattern is shown for a clamped circular plate under uniform pressure with both GBL and GAL set at 9.54 lpi. In Fig. 4-(b) the moiré pattern was obtained with GAL changed to 11.46 lpi while GBL was kept the same. It is seen that along the horizontal diameter the fringe density at the central portion was increased by the use of linear mismatch whereas the fringe densities at both ends were reduced. It was of course expected because the circular plate was bent in such a way that the curvature at the central portion had sign different from that of the end portions. The shape of the plate is schematically shown in Fig. 2. If we denote convex curvature as positive, using the camera as center, then the linear mismatch of the type shown in Fig. 4-(b) can be defined as positive. Since it (the fictitious curvature represented by the mismatch) had the same sign as that

of the flexed plate at the central region, it increased the number of fringes there. In order to increase the fringe density at the end portions it is evident that a (linear) mismatch of opposite sign must be used. An example is given in Fig. 5 where (a) depicts a moiré pattern of the same plate under the same load as in Fig. 4 but with grating lines changed to 11.46 lpi for both GBL and GAL. In Fig. 5(b) a (linear) mismatch of GBL=9.54 lpi and GAL=11.46 lpi was introduced. The mismatch is of the same magnitude but opposite sign as that of the pattern in Fig. 4(b). It is seen, by comparing Fig. 5(b) with Fig. 5(a), that the fringe densities at the end portions were increased whereas that at the central portion decreased. The linear mismatch of the type as in Fig. 5(b) is then called negative according to the convention set earlier. The moiré pattern corresponding to the (linear) mismatches introduced in Fig. 4(b) as 5(b) is shown in Fig. 3(a). It should be noted that the appearance of the fringes does not tell the sign they contain, although the magnitude is represented by the fringe density of the pattern. Since the two mismatches only differ in sign they should have identical moiré patterns.

The slope curves along the horizontal diameter for Figs. 4 and 5 are shown in Fig. 6 and 7, respectively. Three curves each were drawn representing the original load pattern*, the mismatch, and the load plus mismatch pattern, respectively. It is noted that the slope curve can be drawn with much greater accuracy at the central region in Fig. 6 than the original load pattern. The same is true at the end portions in Fig. 7. To retrieve the actual slope , it is only necessary to take the difference between the two curves (the load plus mismatch curve and the mismatch)curve which of

---

* In actual analysis the slope curve of the original load pattern need not be drawn , in general.

course is a straight line). In actual analysis it is usually the curvature that is needed. It is then more convenient to take the difference of the slopes of the slope curves. One alternative is to obtain the entire slope curve for the original load pattern from the two other curves, so that usual procedures of analysis can be applied. This in general would require more than one mismatched patterns, of which each contributes a portion for which the (linear mismatch) is additive.

If we denote the fringe orders of load pattern, mismatch pattern, and load plus mismatch pattern as N_ℓ, N_m, and $N_{\ell+m}$, it is evident that the following equation holds:

$$N_\ell = N_{\ell+m} - N_m \tag{3}$$

If we further denote L_1 and L_2 as the line densities of GBL and GAL respectively, then N_m is positive if $L_2 > L_1$ (i.e. positive linear mismatch), and negative if $L_2 < L_1$ (negative linear mismatch). Eq. (3) can be used for calculating the actual partial slopes at a point or can be used to retrieve the entire slope curves for the actual loading.

The Use of Rotational Mismatch

It is recalled that in solving plate problems curvatures as well as twist are needed. While the former involves the direct derivative of partial slopes (i.e. $\frac{\partial^2 w}{\partial x^2}$, $\frac{\partial^2 w}{\partial y^2}$), the latter derives from cross derivative of partial slopes ($\frac{\partial^2 w}{\partial x \partial y}$). It may be noted in the analysis of using linear mismatches, fringe densities were increased in the direction normal to the grating lines. It is of course expected in view of the nature of linear mismatch fringes as shown in Fig. 3(a), which run parallel to the grating lines. As a result linear mismatch offers no help to the accurate plotting of partial slope curve in the direction parallel to the grating lines.

The rotational mismatch fringes as shown in Fig. 3(b), however, are running almost perpendicular to the grating lines. Their use in the moiré pattern will then increase the fringe densities along the lines. Indeed as shown in Fig. 8, the fringe density along sections perpendicular to the grating lines were considerably increased by the introduction of a rotational mismatch of $\theta = 10.15^{\circ}$. The moiré pattern in Fig. 8(b) is the vectorial sum of the patterns in Fig. 8(a) and Fig. 3(b). The rotational mismatch was introduced by tilting the whole slide projector for the (photographic) exposure of GAL, and the magnitude of the rotational mismatch was obtained by measuring the orientation difference of the grating lines on the ground glass (see Fig. 2). It should be noted that while there is no difference in rotating either GBL or GAL to obtain the rotational mismatch, it is the GBL that should be used for analysis, i.e. its principal direction is the direction along which the partial slopes are represented by the moiré fringes.

An example is given in Fig. 9 showing the improvement that rotational mismatch renders for the accurate obtaining of twist. The slope curves along a vertical section 0.6" to the left of the diameter was drawn for the

load (moiré) pattern, mismatch (moiré) pattern, and load plus mismatch (moiré) pattern. The slope curve for the load pattern (which has three points to define, if using dark fringes) could not possibly be drawn with any accuracy without the help of mismatch and load plus mismatch patterns (each of which has more than ten points to define the slope curve). In order for rotational mismatch technique to be effective, the imposed rotation should have the same sign as that of the actual rotation of the grating due to loading. Otherwise the fringe density will decrease rather than increase as evidenced by the nearly zero fringe density at the corners in the second and fourth quadrants of the moiré pattern in Fig. 8(b). As in the case of linear mismatch technique rotational mismatches of opposite signs should be introduced, if necessary, to help local regions in need of higher fringe density. The final slope curves are obtained by taking the algebraic difference of the slope curves of the load plus mismatch pattern and the mismatch pattern. The rotational mismatch is defined as positive if it has the same sign as that of the local rotation of the grating, and negative if opposite. In an analogous way, a pattern of rotational mismatch as shown in Fig. 3(b) may be considered as a uniform fictitious twist field. Its use for the accurate obtaining of twists of a flexed plate is the same as that of a pattern of linear mismatch for the accurate obtaining of curvatures of a flexed plate.

There are other uses of rotational mismatches. When too fine a grating is used so that the moiré fringes tend to lose their definition or when other types of fringes start to form in some portions of the pattern, the use of rotational mismatch often results in a better picture. As shown in Fig. 1(c) where the moiré pattern was obtained by adding a rotational mismatch of 10.15° into the pattern of Fig. 1(b). It is seen that the fringes at the central region in Fig. 1(c) are much more clearly defined than that in Fig. 1(b).

in which poor definition was caused by the crowding of fringes as well as the forming of another set of fringes. This set of fringes is also more visible in Fig. 1(c), but intersecting the fringes of partial slopes at such an angle that they are distinguishable from each other.

Yet another application of rotational mismatch is its use for obtaining moiré of moiré patterns as discussed by Beranek [9].

The Combinational Use of Both Types of Mismatches

It is evident that both linear and rotational mismatches can be introduced into a moiré pattern simultaneously. As a result fringe densities along directions perpendicular and parallel to the grating lines can both be increased so that curvatures as well as twist can be obtained with better accuracy. Examples are shown in Fig. 10 where Fig. 10(a) shows a pattern of load and negative linear mismatch and an anti-clockwise rotational mismatch and Fig. 10(b) a positive linear mismatch and an anti-clockwise rotational mismatch. The load was the same as in the previous cases. It should be noted that the geometry of the model and the loading were such that the original (no mismatch) moiré pattern was symmetrical with respect to the vertical diameter. Therefore, introducing a rotational mismatch of opposite sign would merely change the pattern in such a way that the left and right-hand sides were interchanged.

It is seen that with the application of both linear and rotational mismatches, fringe densities along vertical as well as horizontal directions were increased in the patterns. The pattern in Fig. 10(a) is the vectorial combination of patterns in Fig. 5(b) and Fig. 3(b) whereas the pattern in Fig. 10(b) is the vectorial combination of patterns in Fig. 4(b) and Fig.3(b).

In general, with the use of combinational mismatches, a better balanced moiré pattern is obtained in the sense that there is no "poor" regions where a mismatch of opposite sign (be it linear or rotational) should be introduced as is the case in Fig. 4(b), 5(b) and 8(b). While it is true that a mismatch of any type, if the magnitude is large enough, would result in a pattern having dense fringes everywhere, there exists the danger of overcrowding somewhere in the field that a second set of fringes may be formed. This is one of the things that the proposed mismatch technique is

trying to prevent in the first place. Therefore it may be stated that while either linear or rotational mismatch can be used alone to improve a moiré pattern (usually a region of it), the combinational use of linear and rotational mismatches is preferred if overall improvement of the whole pattern is desired.

Conclusion

It may be concluded that the mismatch technique can be used effectively to improve the accuracy of Ligtenberg's reflective moiré method for plates. Linear mismatch is equivalent to a field of fictitious curvature whereas rotational mismatch corresponds to a fictitious twist field. The mismatches can be used either individually or combinationally. If the improvement of overall fringe density of a pattern is needed, it is preferable to use both linear and rotational mismatches.

Acknowledgement

The authors would like to acknowledge gratefully the financial support of the National Science Foundation through grant No. GK-23007.

References

1. Ligtenberg, F.K., "The Moiré Method: A New Experimental Method for the Determination of Moments in Small Slab Models". Proc. SESA Vol. 12, No. 2, 1954, pp. 83-98.

2. Vreedenburgh, C.G.J., and Van Wijngaarden, H., "New Progress in Our Knowledge About the Moment Distribution in Flat Slabs by Means of the Moire Method". Proc. SESA Vol. 12, No. 2, 1954, pp. 99-114.

3. Bouwkamp, J.G., "Analysis of Two-Dimensional Stress Problems by the Moiré Method", Proceedings of the First International Congress of Experimental Mechanics, New York, 1963. pp. 195-218.

4. Rieder, G. and Ritter, R. "Krümmungsmessung an belasteten Platten nach dem Ligtenbergschen Moiré-Verfahren," Forschung im Ingenieur-Wessen, VDI-Verlag Dusseldorf, Vol. 31, No. 2, 1965, pp. 33-44.

5. Chiang, Fu-pen and Treiber, J., "A Note on Ligtenberg's Reflective Moiré Method," Experimental Mechanics, in press.

6. De Haas, H.M. and Loof, H.W., "An Optical Method to Facilitate the Interpretation of Moiré Pictures," VDI-Berichte, Nr. 102, Experimentelle Spannunzsanlyse, Berlin, 1966, pp. 65-70.

7. Chiang, Fu-pen, "Techniques of Optical Spatial Filtering Applied to the Processing of Moiré Fringe Patterns," Experimental Mechanics , Vol. 9, No. 11, Nov. 1969. pp. 523-526.

8. Chiang, Fu-pen, "A Method to Increase the Accuracy of Moiré Method," J. of the Eng. Mech. Div. Proc. ASCE, Vol. 91, No. EMI. Feb. 1965, pp. 137-149.

9. Beranek, W.J., "Rapid Interpretation of Moiré Photographs," Experimental Mechanics Vol. 8 No. 6. 1968 pp. 249-256.

10. Morse, S., Durelli, A.J., and Sciammarella, C.A., "Geometry of Moiré Fringes in Strain Analysis," J. of Eng. Mech. Div. Proc. ASCE Vol. 86 No. EM4, 1960, pp. 105-126.

Figure Captions

1. Moiré Patterns of a Clamped Circular Plate Under Uniform Pressure Showing the Effect of Grating Being too Fine.
   (a) GBL = GAL = 9.54 lpi
   (b) GBL = GAL = 17.7 lpi
   (c) GBL = GAL = 17.7 lpi and $\theta = 10.15^{\circ}$ (counterclockwise).

2. Optical Arrangement of the Modified Ligtenberg's Method for Facilitating the Introduction of Mismatches.

3. Examples of Mismatch Moiré Fringes
   (a) Linear Mismatch
   GBL(GAL) = 9.54 lpi, GAL(GBL) = 11.46 lpi
   (b) Rotational Mismatch
   GBL = GAL = 11.46 lpi, $\theta = 10.15^{\circ}$ (counterclockwise)
   (c) = (a) + (b)

4. Moiré Patterns Showing the Application of Positive Linear Mismatch
   (a) GBL = GAL = 9.54 lpi
   (b) GBL = 11.46 lpi, GAL = 9.54 lpi

5. Moiré Patterns Showing the Application of Negative Linear Mismatch
   (a) GBL = GAL = 11.46 lpi
   (b) GBL = 9.54 lpi, GAL = 11.46 lpi

6. Partial Slope Curves along Horizontal Diameter of the Circular Plate from Patterns in Fig. 4 and Fig. 3(a).

7. Partial Slope Curves along Horizontal Diameter of the Circular Plate from Patterns in Fig. 5 and Fig. 3(a).

8. Moiré Patterns Showing the Application of Rotational Mismatch
   (a) GBL = GAL = 11.46 lpi
   (b) GBL = GAL = 11.46 lpi, $\theta = 10.15^{\circ}$ (counterclockwise)

9. Partial Slope Curves along Section A-A of the Circular Plate From Patterns in Fig. 8 and Fig. 3(b).

10. Moiré Patterns Showing the Application of Combined Linear and Rotational Mismatches

   (a) GBL = 9.54 lpi, GAL = 11.46 lpi, $\theta = 10.15^{\circ}$ (counterclockwise)
   (b) GBL = 11.46 lpi, GAL = 9.54 lpi, $\theta = 10.15^{\circ}$ (counterclockwise)

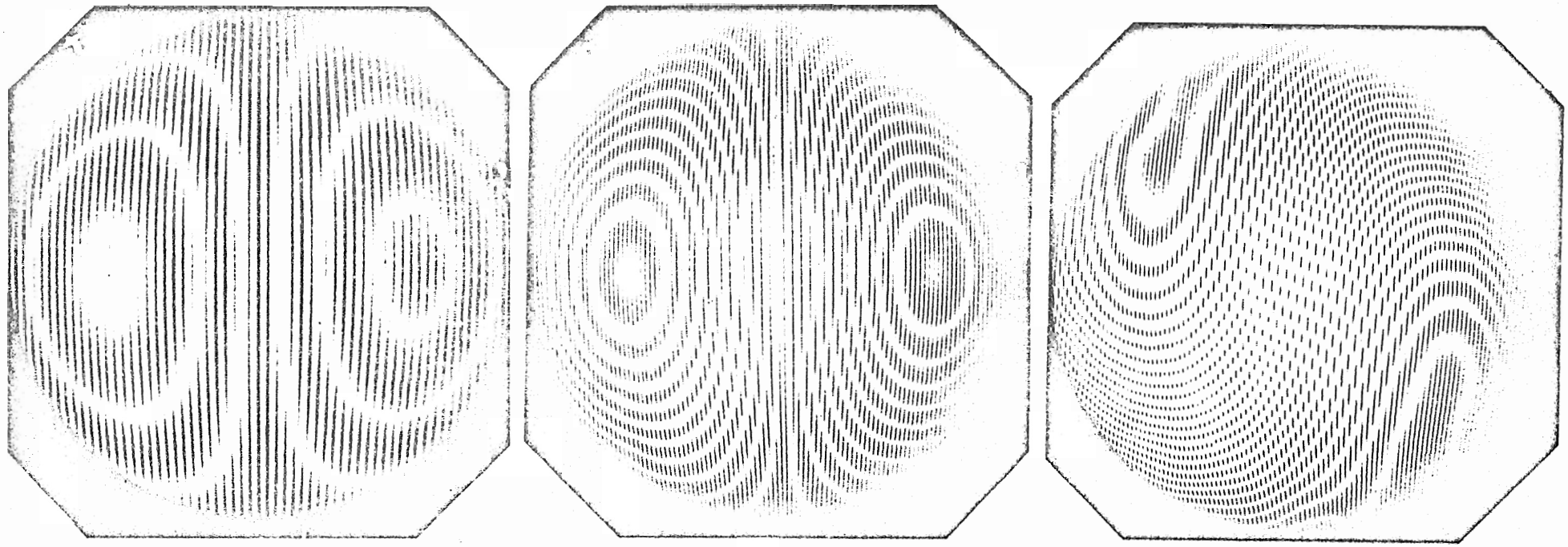

1. Moiré Patterns of a Clamped Circular Plate Under Uniform Pressure Showing the Effect of Grating Being too Fine.
   (a) $G_1L = G_2L = 9.54$ lpi
   (b) $G_1L = G_2L = 17.7$ lpi
   (c) $G_1L = G_2L = 17.7$ lpi and $\theta = 10.15^{\circ}$ (counterclockwise).

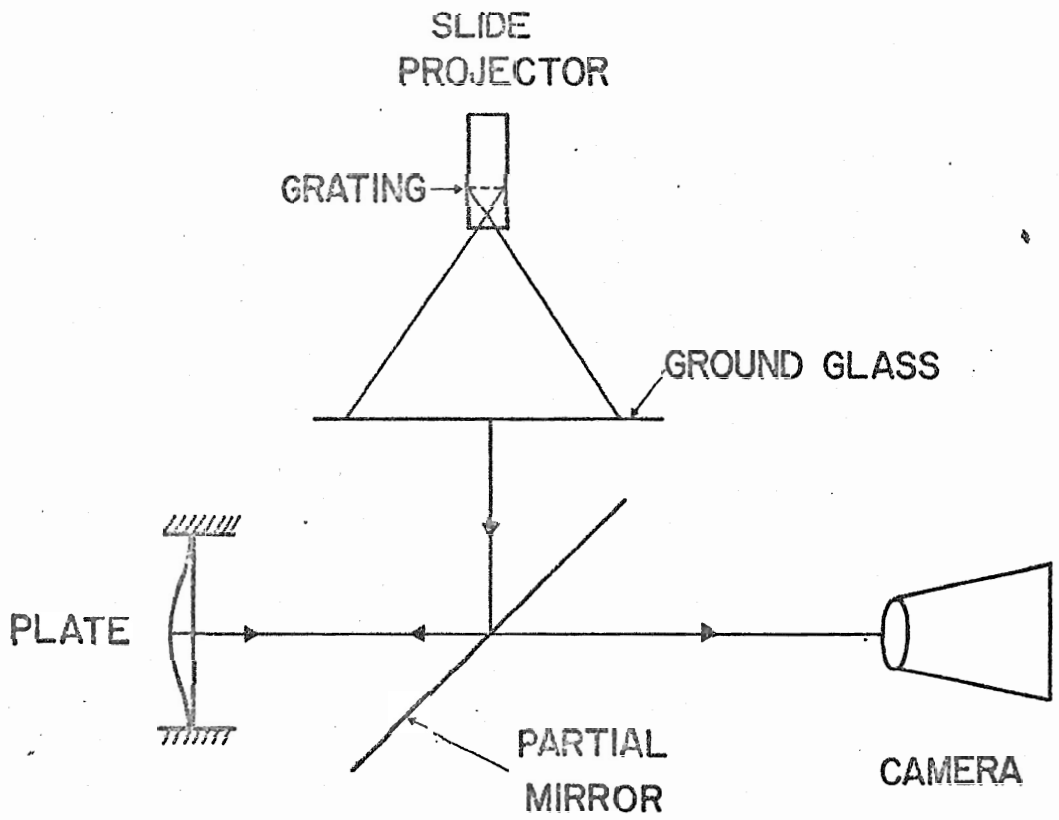

2. Optical Arrangement of the Modified Liptenberg's Method for Facilitating the Introduction of Mismatches.

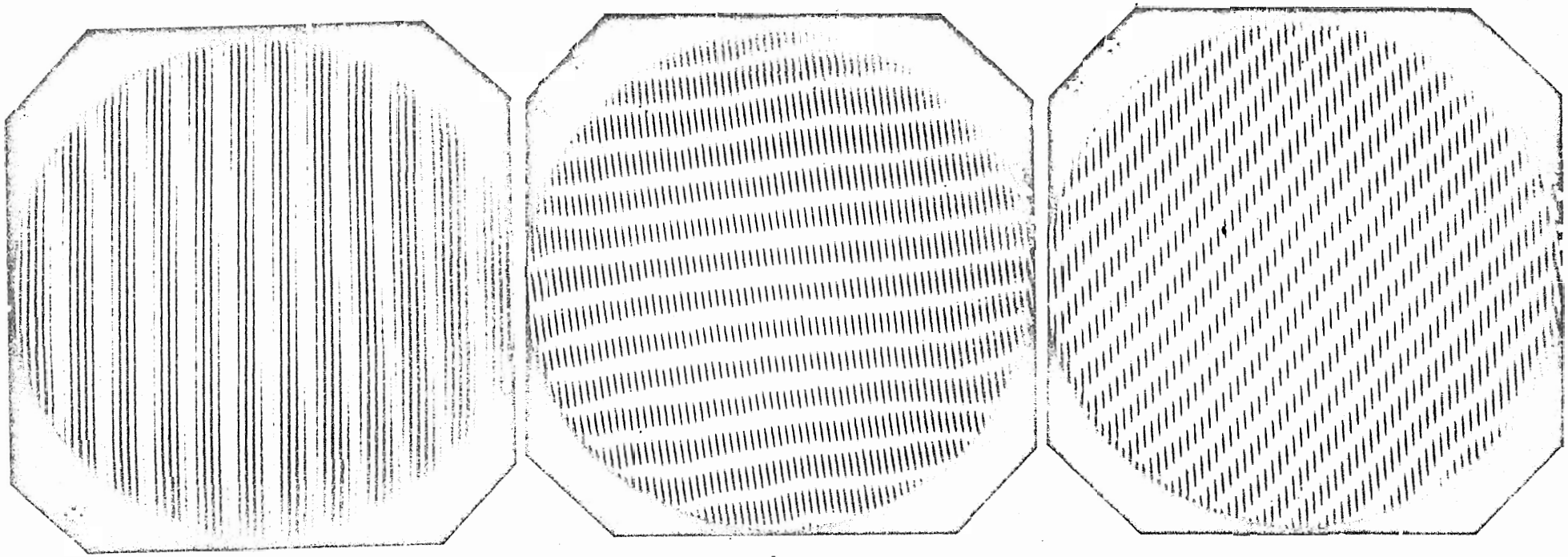

(a) (b) (c)

3. Examples of Mismatch Moiré Fringes
   (a) Linear Mismatch
       GBL(GAL) = 9.54 lpi, GAL(GBL) = 11.46 lpi
   (b) Rotational Mismatch
       GBL = GAL = 11.46 lpi, $\theta = 10.15^{\circ}$ (counterclockwise)
   (c) = (a) + (b)

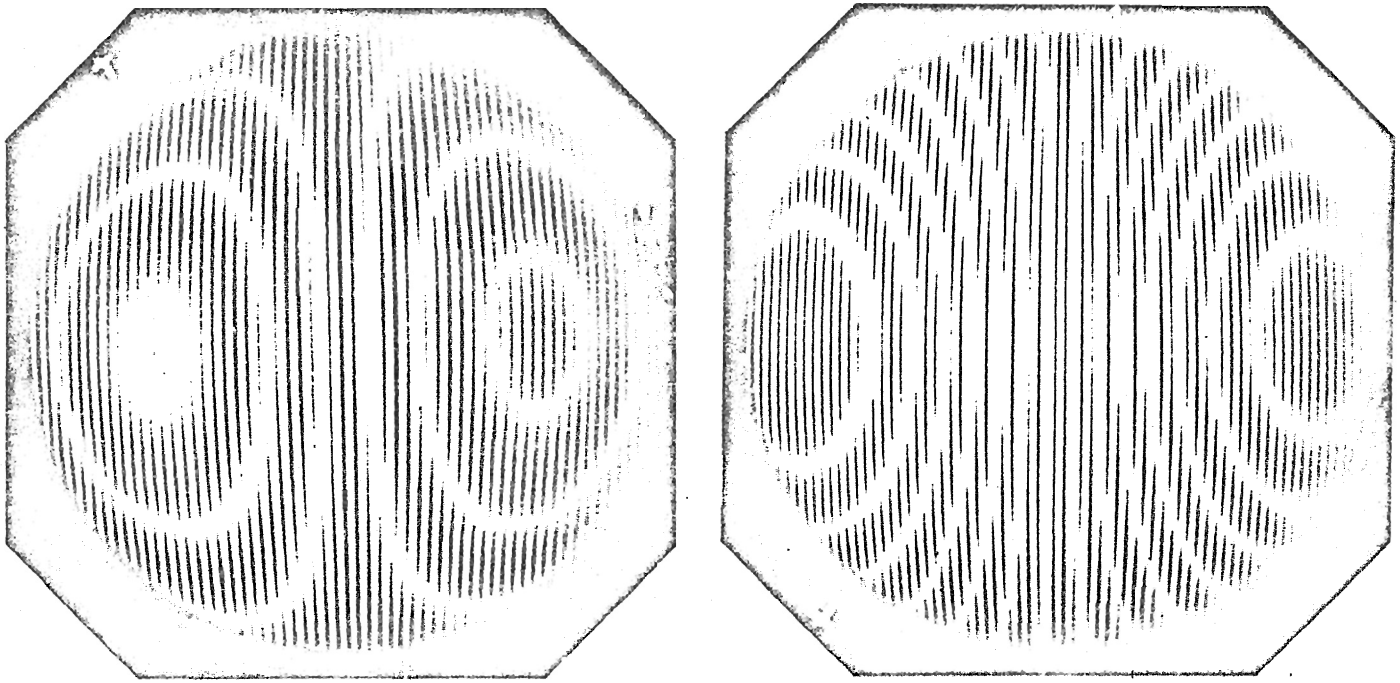

8. Moiré Patterns Showing the Application of Positive Linear Mismatch
   (a) GBL = GAL = 9.54 lpi
   (b) GBL = 10.46 lpi, GAL = 9.54 lpi

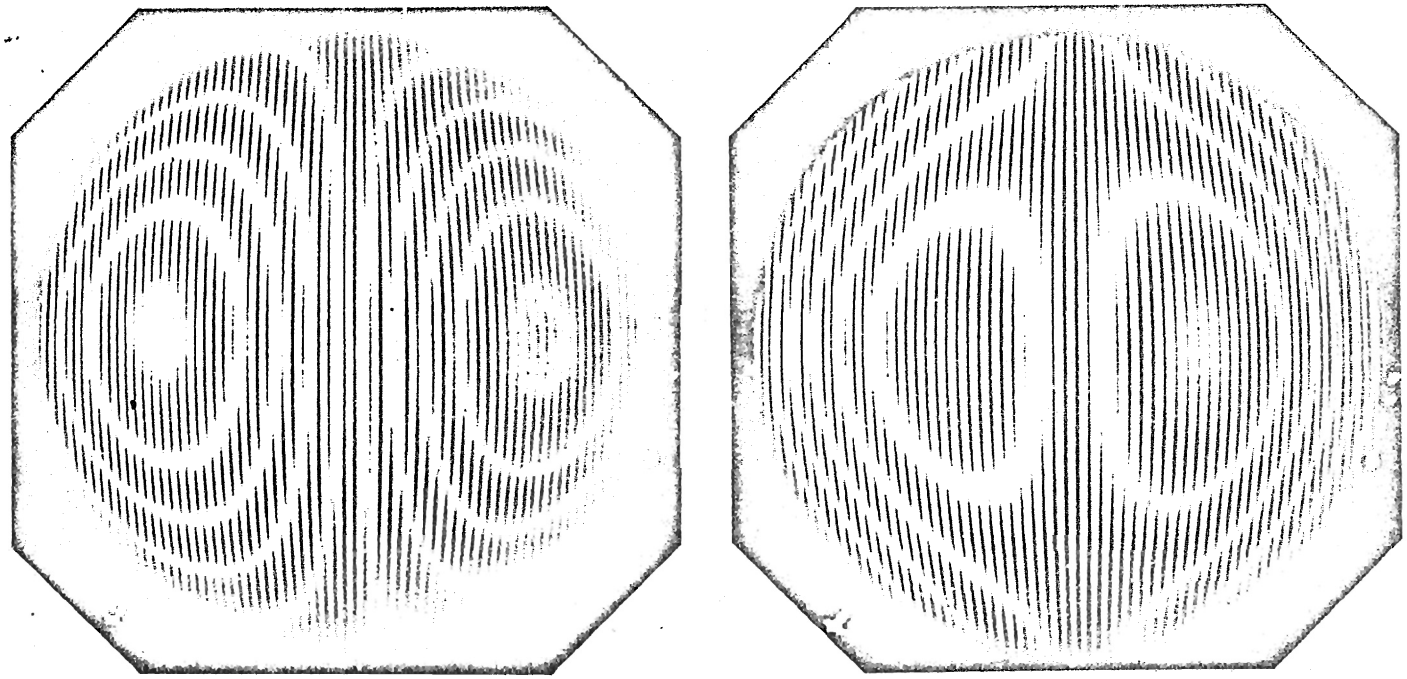

5. Moiré Patterns Showing the Application of Negative Linear Mismatch
   (a) GBL = GAL = 11.46 lpi
   (b) GBL = 9.54 lpi, GAL = 11.46 lpi

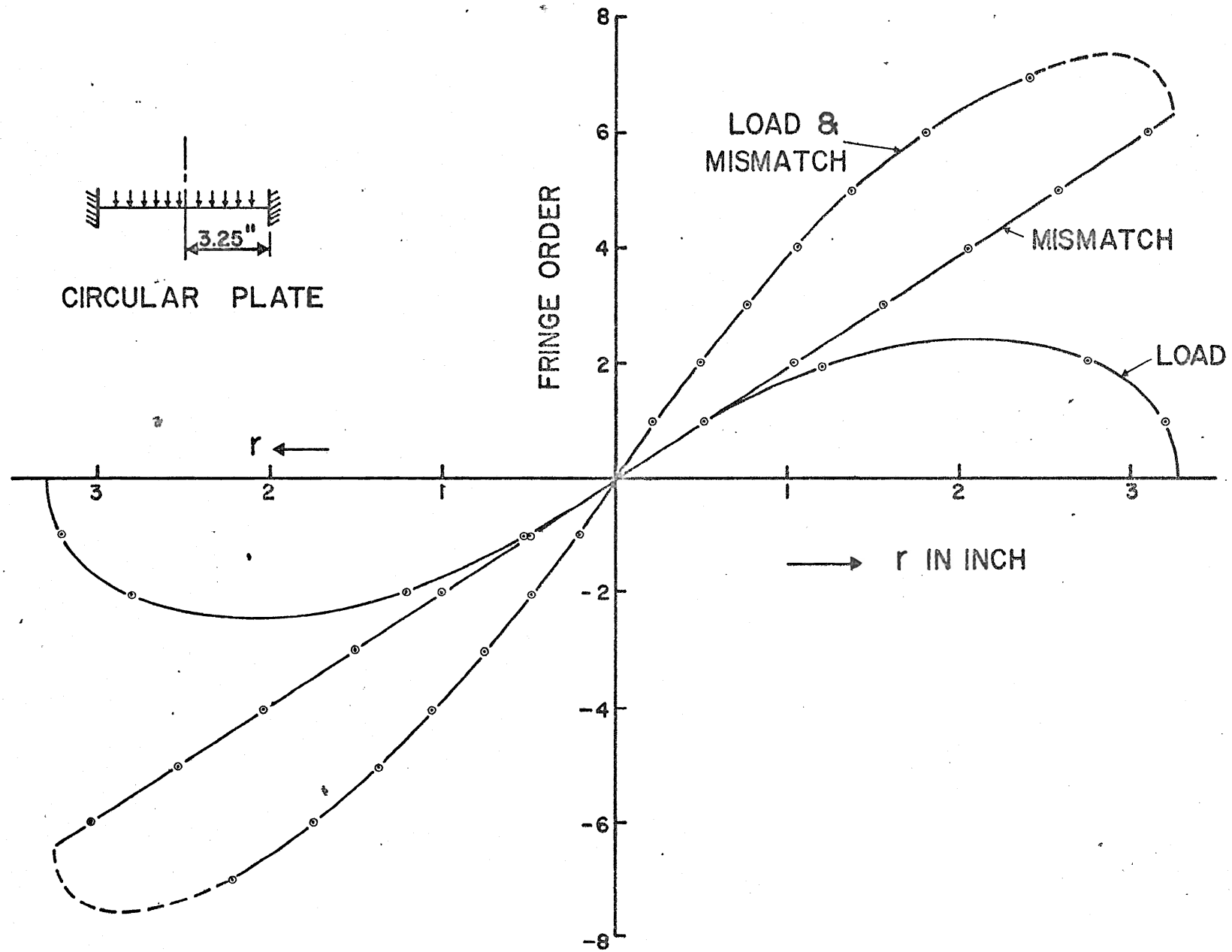

6. Partial Slope Curves along Horizontal Diameter of the Circular Plate from Patterns in Fig. 4 and Fig. 3(a).

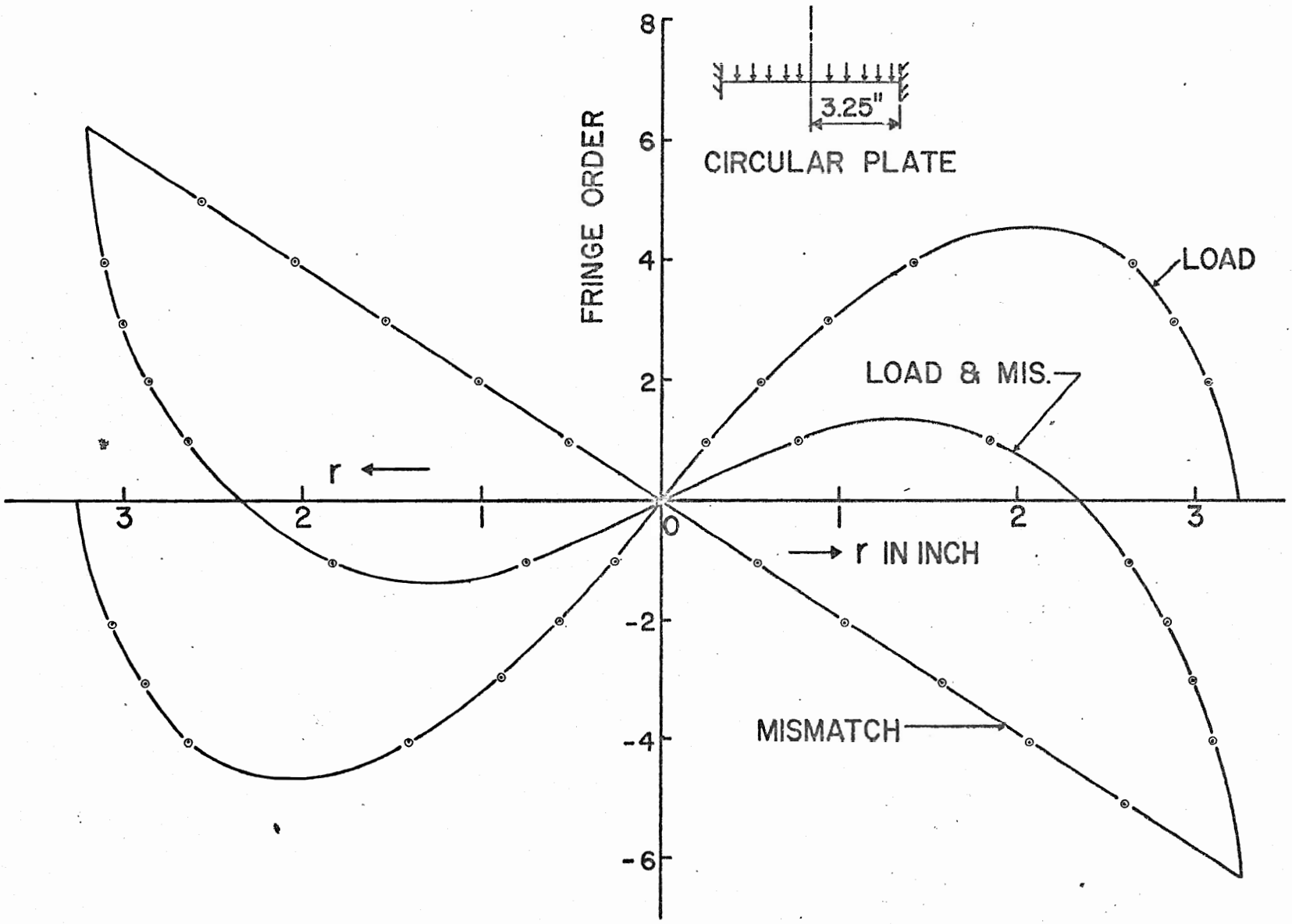

7. Partial Slope Curves along Horizontal Diameter of the Circular Plate from Patterns in Fig. 5 and Fig. 3(a).

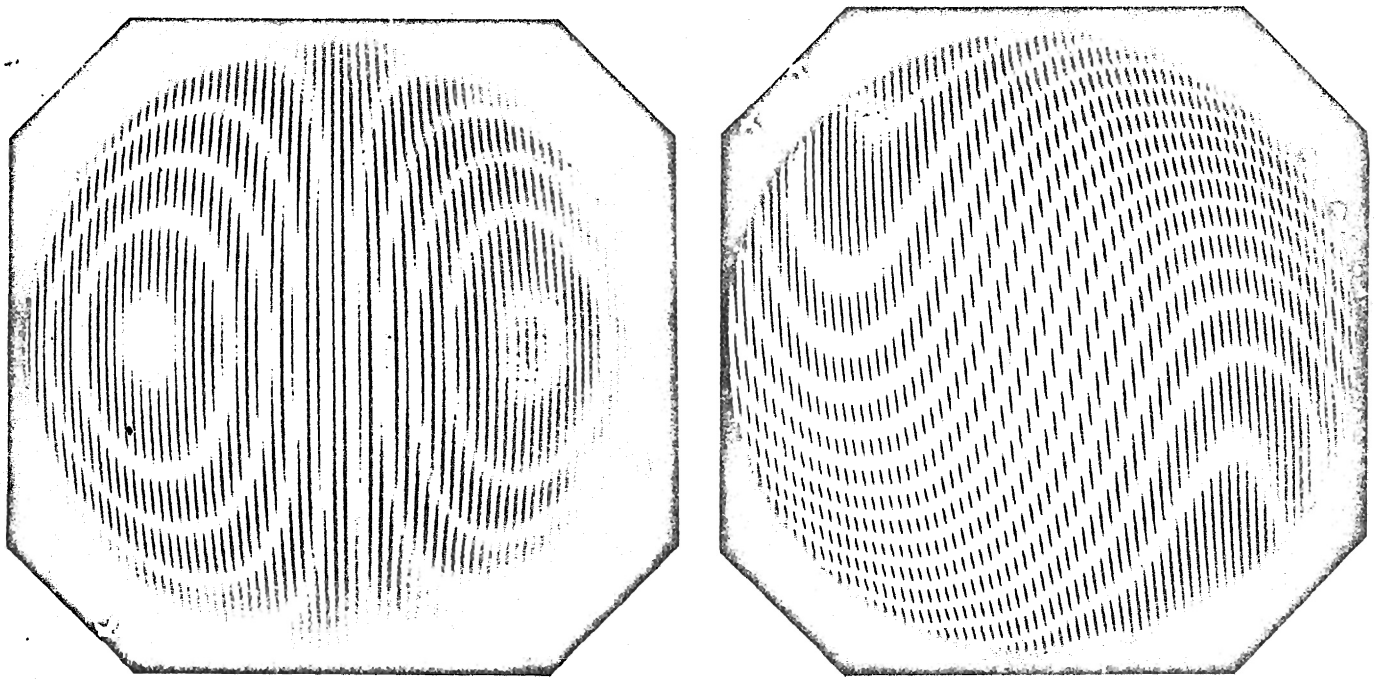

8. Moiré Patterns Showing the Application of Rotational Mismatch
   (a) GBL = GAL = 11.46 lpi
   (b) GBL = GAL = 11.46 lpi, θ = 10.15^{o} (counterclockwise)

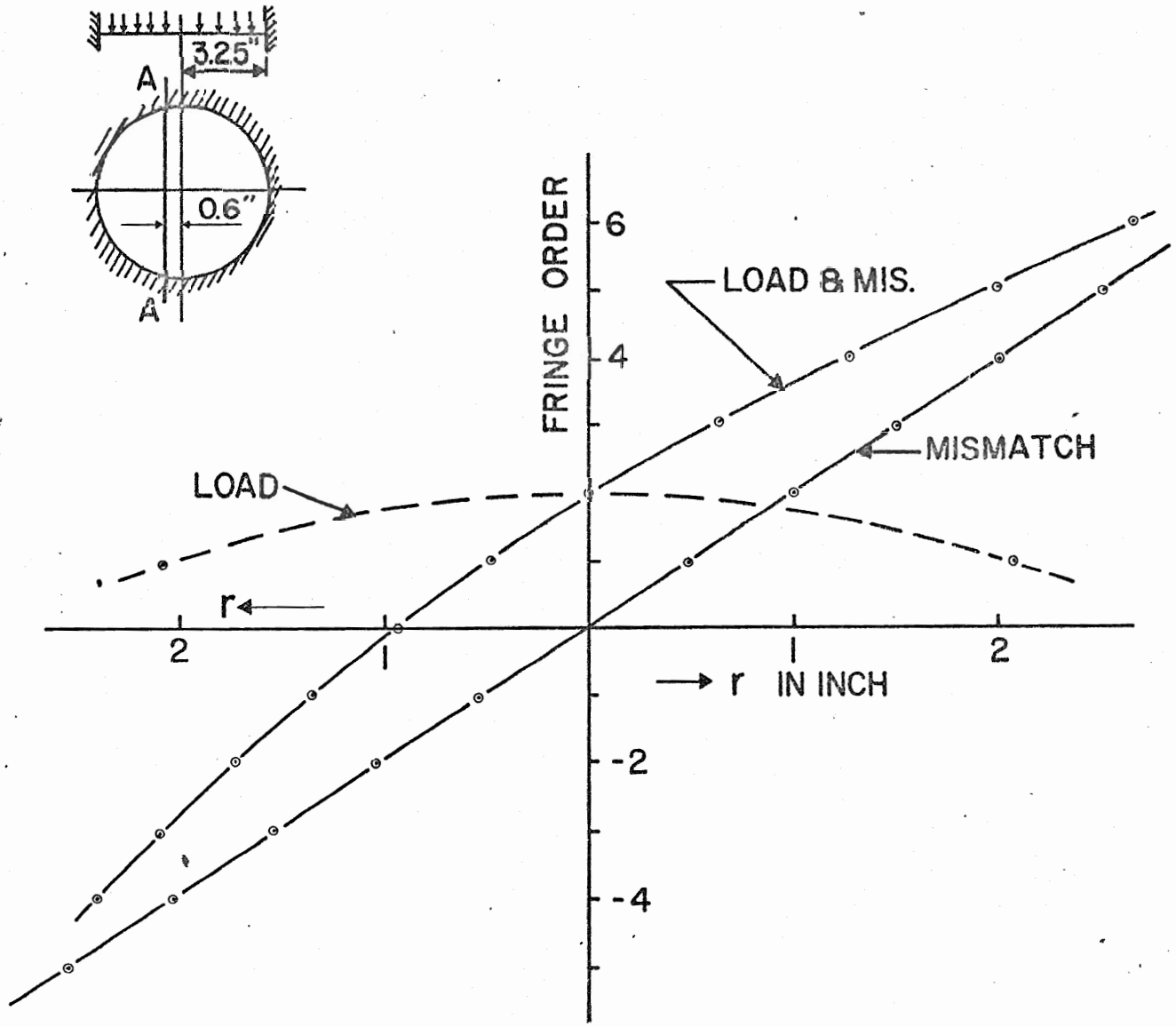

9. Partial Slope Curves along Section A-A of the Circular Plate From Patterns in Fig. 8 and Fig. 3(b).

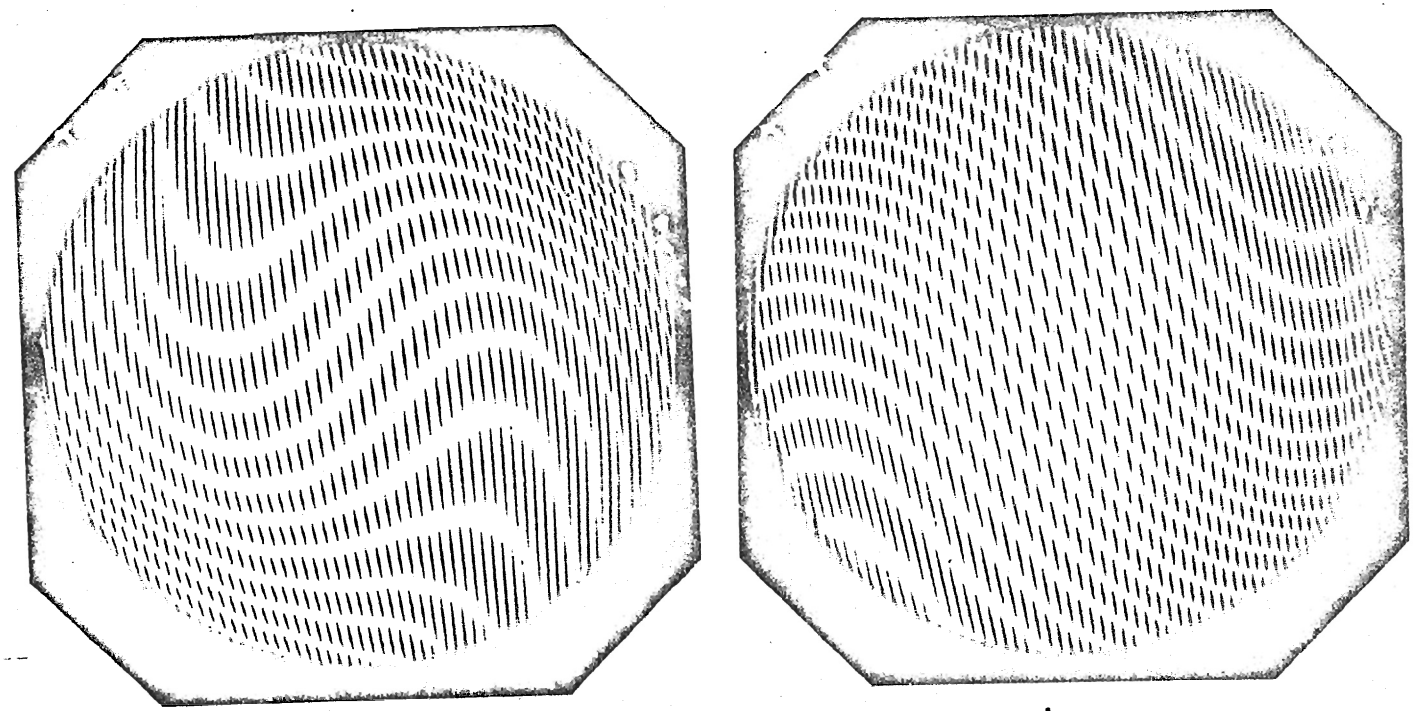

10. Moiré Patterns Showing the Application of Combined Linear and Rotational Mismatches

(a) GBL = 9.54 lpi, GAL = 11.46 lpi, $\theta = 10.15^{\circ}$ (counterclockwise)
(b) GBL = 11.46 lpi, GAL = 9.54 lpi, $\theta = 10.15^{\circ}$ (counterclockwise)